AERE - R 10045

AERE - R 10045

United Kingdom Atomic Energy Authority

HARWELL

The Influence of Electronic Straggling on Range Distributions of Energetic Ions

N.E.B. Cowern
Nuclear Physics Division
AERE Harwell, Oxfordshire
February 1981

APPROVED FOR PUBLICATION

AERE-R10045

The influence of electronic straggling on range distributions of energetic ions

N.E.B. Cowern

ABSTRACT

The range straggling of ions above the stopping power maximum is shown in a large class of ion-target combinations to include a strong contribution from electronic collisions. Existing calculations based purely on the statistics of nuclear collisions may therefore have underestimated the true range straggling.

The relative contributions of electronic and nuclear collisions are considered in the case of high incident ion energies, and a detailed prediction of the electronic contribution as a function of incident energy is given for the example of ^{4}He in a carbon target.

Nuclear Physics Division,
A.E.R.E., Harwell.

February 1981

HL.81/342

CONTENTS

ILLUSTRATIONS

Fig. 1 Contour plot of the estimated percentage increase I in path length straggling when electronic straggling is included, for high incident ion energies. Ordinate: incident ion mass M_1. Abscissa: target atomic mass M_2. In the region above the line $M_1 = M_2$, the plot also represents the percentage increase I_p in projected range straggling, but below that line the plot overestimates I_p. The cross indicates the ion-target combination ^{4}He on C studied in this paper.

Fig. 2 Energy straggling of ^{4}He in C as a function of ^{4}He energy, used in electronic range straggling evaluation. Solid line at high energy: Bethe-Livingston theory. Solid line at low energy: Chu-Mayer theory. Dashed line: matching curve for intermediate region. Ω_B is the value of Ω_e when the target electrons are treated as free, as in eq. (1).

Fig. 3 Projected range straggling of ^{4}He in C as a function of ^{4}He incident energy. Chained line: nuclear component calculated by Littmark and Ziegler. Dashed line: electronic component calculated in this paper. Solid line: total projected range straggling.

1. Introduction

The experimental and theoretical study of ion range distributions has in the past been mainly confined to energies below the stopping power maximum. This is partly due to the strong theoretical impetus provided by the work of Lindhard et al.[1,2], and partly in response to the technology of ion implantation in semiconductors. The recent application of ion beams to more general materials problems has increasingly involved the use of higher energy beams. The uses of range distribution data in this and other applications are highly diverse: for example, the longitudinal range straggling determines the volume density of ions implanted by a mono-energetic incident beam, it affects the thickness of 'catcher' foil required for depth profiling by the elastic recoil technique, and in nuclear physics it limits the energy resolution when range-energy relations are used to determine energies of reaction products.

In their influential paper dealing with the range distributions of low energy ions Lindhard et al.[1] argued that electronic energy loss fluctuations had a negligible effect on range distributions, and they calculated the range straggling as arising purely from the statistics of elastic nuclear collisions. Since then, several tabulations of ion range distributions at energies at and below the stopping power maximum have been published[3,4,5], all of which have neglected electronic straggling. Recently, Littmark and Ziegler[6] have greatly extended the energy range by describing range distributions up to 1000 MeV for a wide variety of ions, but the effect of electronic straggling was again neglected. On the other hand the range straggling of high energy charged particles in nuclear emulsion and other materials has been treated in earlier work purely in terms of electronic straggling[7,8]. In view of the increasing importance of higher energies in ion beam analysis of materials, it is worthwhile to look again at the relative contributions of nuclear and electronic straggling to range distributions.

2. Range straggling at high energy

As a preliminary it is convenient to consider straggling in the total ion path length, in the (non-relativistic) limit of high incident energy. Here the target nuclei and electrons can be treated as free, and the ion-electron and ion-nucleus scattering cross sections may be treated as Rutherford[9,1]. This yields values for the straggling variances arising from electronic and nuclear energy loss fluctuations which are respectively

$$\eta_e^2 = \Omega_e^2 x = 4\pi e^4 z_1^2 z_2 x \tag{1}$$

$$\eta_n^2 = \Omega_n^2 x = 4\pi e^4 z_1^2 z_2^2 \left(\frac{M_1}{M_1+M_2}\right)^2 x \tag{2}$$

Here z_1, M_1 and z_2, M_2 are the atomic numbers and masses of the ion and target respectively, e is the electronic charge, and x is the distance (in atoms per unit area) travelled through the target. Ω_e^2 and Ω_n^2 are the second moments of the electronic and nuclear single-collision energy loss spectra.

The resulting path length straggling is given to first order by[1]

$$(\Delta R)^2 = \int_0^{E_0} \frac{\Omega 2}{(dE/dx)^3}\, dE \tag{3}$$

$$\Omega^2 = \Omega_e^2 + \Omega_n^2 \tag{3a}$$

where E is the ion energy, initially E_0, and dE/dx is the stopping power at energy E. Eq. (3a) follows from the usual assumption that the occurrence of an electronic collision does not affect the probability of a subsequent nuclear collision and vice versa. The fall in stopping power at high energy ensures that the integral is dominated by high energy straggling as given by eqs. (1) and (2). Since it is usual to neglect Ω_e^2 in range distribution calculations we consider here the effect on the calculated path length straggling of including Ω_e. This produces a fractional increase in path length straggling of $(1 + \Omega_e^2/\Omega_n^2)^{\frac{1}{2}} - 1$. The percentage increase I is shown

in Fig. 1 as a function of M_1 and M_2, with the approximation $M_2 \simeq 2z_2$. Clearly for a wide range of ions and targets, the high energy path length straggling is significantly dependent on electronic straggling.

In practical applications, the projected range straggling ΔR_p is more important than the path length straggling. Owing to large angle scattering in nuclear collisions, the relative contribution of nuclear straggling to the projected range straggling is increased. In approximate calculations of Ω_n such as are needed for estimating the quantity I, this effect can be neglected when $M_1 \geq M_2$. However for $M_1 < M_2$ the effect leads to a reduction in I. Thus Fig. 1 gives useful estimates of I above the line $M_1 = M_2$, but overestimates this quantity for ion-target combinations below the line. Consequently a more detailed approach to the nuclear straggling contribution is necessary. It is also important to discover the dependence of electronic straggling on the incident ion energy, since at sufficiently low incident energies nuclear straggling is known to dominate.

3. Case study of ^{4}He ions in carbon

The projected range straggling has been studied for the case of ^{4}He ions incident on carbon at energies from 1.0 to 100 MeV. Fig. 1 suggests that this example should show a significant increase in range straggling at high incident energy, and thus the transition from the low energy to the high energy situation should be well demonstrated. Since detailed calculations of the nuclear range straggling for energies 1 to 1000 MeV are already available[6] it has been sufficient to calculate the additional contribution from electronic straggling. This calculation is especially simple since almost all ion trajectories above the stopping power maximum are approximately straight. As is shown in the Appendix, the number of trajectories containing large-angle nuclear scatters is sufficently small to have no effect on the electronic straggling contribution. One thus has for the total range straggling variance

$$(\Delta R_p)^2 = (\Delta R_p)_n^2 + (\Delta R_p)_e^2 \quad , \tag{4}$$

where
$$(\Delta R_p)_e^2 = \int_0^{E_0} \frac{\Omega_e^2}{(dE/dx)^3}\, dE \qquad (5)$$

to first order in T/E, where T is the energy loss in a single electronic collision. Since T/E is small this approximation is valid, and a second order[1] computation showed that typical errors in the 1st order calculation were less than 0.01%.

Values for Ω_e^2 above the cut-off energy for target K-shell ionisation were obtained using the Bethe-Livingston theory, following a previously described prescription[10]. At lower energies, the straggling theory of Chu and Mayer[11] was used, and a necessarily arbitrary matching curve was drawn between the two energy regions. Fig. 2 shoes the theoretical straggling curves, and the curve used to match the theoretical values. Values for dE/dx were obtained from the ^{4}He stopping power formulae of Ziegler[12]. The results of the numerical integration for $(\Delta R_p)_e$ (eq.(5)) are shown in Fig. 3, together with the values of $(\Delta R_p)_n$ calculated by Littmark and Ziegler[6] using the same stopping power formulae. Also shown is the resultant total projected range straggling ΔR_p obtained from eq. (4).

As expected, the percentage increase I in ΔR_p due to inclusion of electronic straggling is negligible below 1 MeV, and hence the choice of matching curve used in Fig. 2 is not at all critical. Above 1 MeV the quantity I rises, reaching about 60% at energies above 8 MeV. This value of I is preferable to the prediction of Fig. 1 for ^{4}He in carbon (92%), since we have now correctly used the projected nuclear straggling $(\Delta R_p)_n$ in place of the path length straggling $(\Delta R)_n$. Fig. 1 is still useful at high energy (> about 20 times the energy of the stopping power maximum) for cases where $M_1 \geq M_2$.

4. Conclusions

The results presented here emphasize the importance of electronic collisions in determining range distributions. The example of ^{4}He on carbon shows that electronic straggling can be the predominant contributor to projected

range straggling at quite moderate ion energies. It is therefore essential that quantitative predictions of the electronic straggling contribution should be made available for a significant range of ions and targets. Such predictions should be available as a function of energy, since in practical applications the region of varying $(\Delta R_p)_e/(\Delta R_p)_n$ will be of greater relevance than the high energy region where this ratio is constant. Another straggling process which has not been discussed in this report, namely charge exchange[13,14,15], arises in the energy region of interest. Since it may contribute significantly to range distributions of heavy ions, it too deserves attention if reasonably reliable range distributions are to be available above the stopping power maximum.

Acknowledgements

I should like to thank Dr. J.M. Freeman for verifying the numerical calculations leading to Figs. 1 and 3 of this paper. Thanks are also due to C.J. Woods, Dr. C.J. Sofield and Prof. L.B. Bridwell for helpful criticism of the manuscript.

Appendix

The calculation in section 3 of the electronic contribution to ΔR_p for ^4He ions in carbon depended on the assumption of straight line trajectories in the region above the stopping power maximum. This is because the calculation equated $(\Delta R)_e$ to $(\Delta R_p)_e$ and thus ignored any angular deflections which might occur. The approach is reasonable when considering only electronic collisions which involve very small scattering angles. However, if significant nuclear scattering were present at energies above the stopping power maximum, the projection of $(\Delta R)_e$ along the beam direction would be somewhat reduced. It is therefore important to determine the extent of nuclear scattering at angles greater than $\sim 10^o$. This angle is chosen since simple geometrical considerations show that for a scattering angle of 10^o or less occurring at some point within the ion trajectory, the percentage reduction in $(\Delta R_p)_e$ would be less than $100(1 - \cos 10^o) = 1.5\%$.

We therefore consider the probability P of a nuclear collision occurring with a laboratory scattering angle $\geq \theta_o$, when an ion of charge z_1 and atomic mass M_1 slows down from an initial energy E_i to a final energy E_f. Since our energy region of interest stretches upward from the stopping maximum to much higher energies, an approximate treatment can be achieved as follows.

1. The ion stopping power is described by the simple Bethe theory without shell or other corrections. Thus

$$-\frac{dE}{dx} = \frac{4\pi e^4 z_1^2 z_2}{(2m_e/M_1)E} \ln\left(\frac{4m_e}{M_1 I}.E\right) \qquad (6)$$

where M_2, z_2, I are respectively the atomic mass, charge, and mean ionisation energy of the target atoms, and m_e is the electron mass.

2. The ion-target nuclear scattering potential is treated as Coulombic, leading to Rutherford scattering. It is convenient to use the formula[16]

$$\frac{d\sigma}{d\Omega} = 1.296 \frac{(z_1 z_2)^2}{E^2} \left[\text{cosec}^4 \frac{\theta}{2} - 2\left(\frac{M_1}{M_2}\right)^2 + \ldots\right] \text{ mb/steradian} \qquad (7)$$

valid only for $M_1 < M_2$, where θ is the laboratory scattering angle, Ω is the solid angle in the laboratory frame, and E is in MeV. The restriction to $M_1 < M_2$ is of no consequence because scattering effects in range straggling are of minor importance when $M_1 \geq M_2$.

The cross section $\sigma_{\theta_\circ}$ for collision with a scattering angle $\geq \theta_\circ$ is obtained by integration of eq. (7).

$$\sigma_{\theta_\circ} = \int_{\theta=\theta_\circ}^{\pi} d\sigma = \int_{\theta_\circ}^{\pi} 2\pi \sin\theta \left(\frac{d\sigma}{d\Omega}\right) d\theta$$

$$= 1.296 \frac{(z_1 z_2)^2}{E^2} \cdot 4\pi \left[\cot^2 \frac{\theta_\circ}{2} - 2 \left(\frac{M_1}{M_2}\right) \cos^2 \frac{\theta_\circ}{2}\right] \qquad (8)$$

neglecting higher order terms in $\left(\frac{M_1}{M_2}\right)^2$.

The probability P of a collision with $\theta \geq \theta_\circ$ in slowing down from E_i to E_f (provided it is small) is

$$P = \int_{E_i}^{E_f} \sigma_{\theta_\circ} \left(\frac{dE}{dx}\right)^{-1} dE \qquad (9)$$

which from eqs. (6) and (8) is

$$P = 1.371 \times 10^{-6} \frac{z_2}{M_1} \left[\tfrac{1}{2} \cot^2 \frac{\theta_\circ}{2} - \left(\frac{M_1}{M_2}\right)^2 \cos^2 \frac{\theta_\circ}{2}\right] \int_{E_f}^{E_i} \frac{dE}{E \ell n c E} \qquad (10)$$

where $c = 4m_e/M_1 I$.

Solution of the integral in eq. (10) yields

$$P = 1.371 \times 10^{-6} z_2 / M_1 \left[\tfrac{1}{2} \cot^2 \frac{\theta_\circ}{2} - \left(\frac{M_1}{M_2}\right)^2 \cos^2 \frac{\theta_\circ}{2}\right] (\ell n \ell n\, cE_i - \ell n \ell n c E_f)$$

This result indicates that for almost all ion-target combinations the probability of a scatter > 10° is negligible for all incident energies of interest, provided E_f is not below the stopping maximum (where $\ell n \ell n\, cE_f$ becomes large

and negative). For example in the case of ^{4}He in carbon considered in this report, the probability of a scatter > 10^{o} in slowing down from 1000 MeV to 1 MeV is estimated as 0.21×10^{-3}. Thus the assumption of linear trajectories made in section 3 is secure.

References

1. J. Lindhard, M. Scharff and H.E. Schiøtt, Mat. Fys. Medd. Dan. Vid. Selsk. 33, No. 14 (1963).
2. H.E. Schiøtt, Mat. Fys. Medd. Dan. Vid. Selsk. 35, No. 9 (1966).
3. J.F. Gibbons, W.S. Johnson and S.W. Mylroie, Projected range statistics (2nd ed., Halstead Press, New York, 1975).
4. D.K. Brice, Vol. 1, Ion implantation range and energy deposition distributions (IFI/Plenum, New York, 1975)
5. K.B. Winterbon, Vol. 2, Ion implantation range and energy deposition distributions (IFI/Plenum, New York, 1975)
6. U. Littmark and J.F. Ziegler, Vol. 6, The stopping and ranges of ions in matter (Pergamon Press, New York, 1980)
7. W.H. Barkas, F.M. Smith and W. Birnbaum, Phys. Rev. 98 (1955) 605.
8. R.M. Sternheimer, Phys. Rev. 117 (1960) 485.
9. N. Bohr, Phil. Mag. 30 (1915) 581.
10. C.J. Sofield, N.E.B. Cowern, J.M. Freeman and K. Parthasaradhi, Phys. Rev. A15 (1977) 2221
11. W.K. Chu, in "Ion beam handbook for materials analysis", ed. J.W. Mayer and E. Rimini, Academic Press, New York, 1977.
12. J.F. Ziegler, Vol. 4, The stopping and ranges of ions in matter, Pergamon Press, New York, 1980).
13. O. Vollmer, Nucl. Instr. and Meth. 121 (1974) 373
14. C.J. Sofield, N.E.B. Cowern, J.R. Petty, J.M. Freeman and J.P. Mason, Phys. Rev. A17 (1978) 859
15. N.E.B. Cowern, C.J. Sofield, J.M. Freeman and J.P. Mason, Phys. Rev. A19 (1979) 111
16. J.B. Marion and F.C. Young, Nuclear Reaction Analysis, North Holland, 1968.

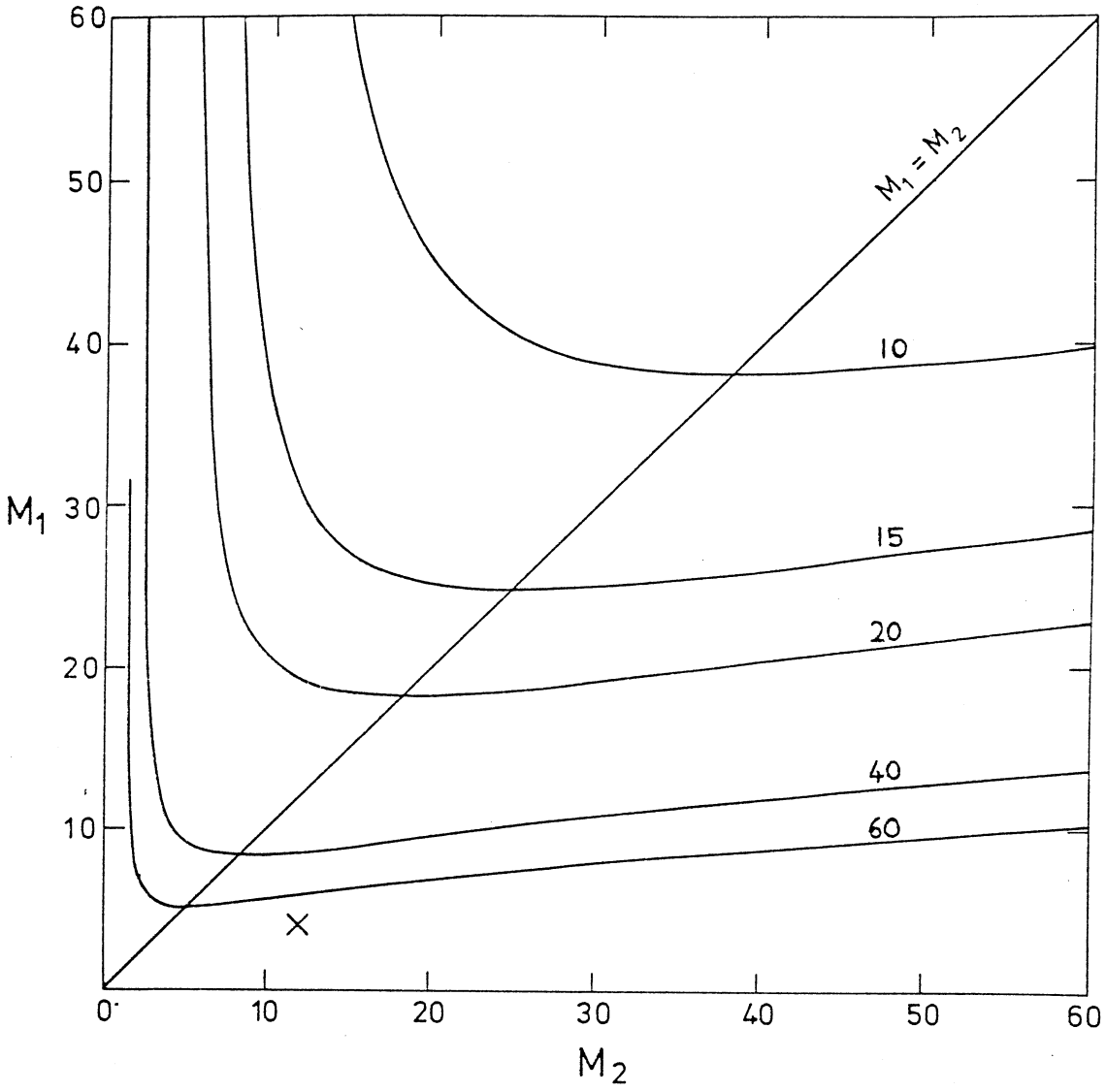

AERE - R 10045 Fig. 1

Contour plot of the estimated percentage increase I in path length straggling when electronic straggling is included, for high incident ion energies. Ordinate: incident ion mass M_1. Abscissa: target atomic mass M_2. In the region above the line $M_1 = M_2$, the plot also represents the percentage increase I_p in projected range straggling, but below that line the plot overestimates I_p. The cross indicates the ion-target combination ^{4}He on C studied in this paper.

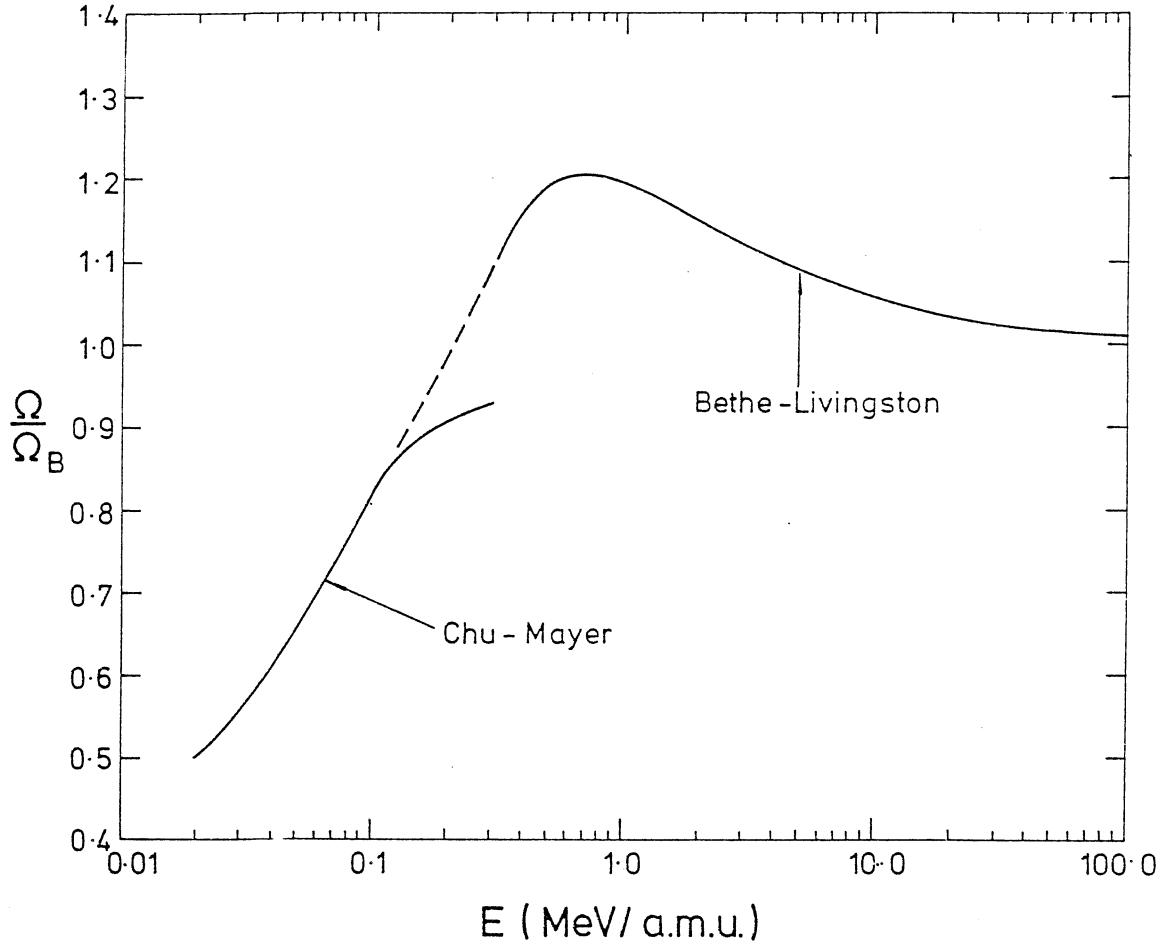

AERE - R 10045 Fig. 2

Energy straggling of ^{4}He in C as a function of ^{4}He energy, used in electronic range straggling evaluation. Solid line at high energy: Bethe-Livingston theory. Solid line at low energy: Chu-Mayer theory. Dashed line: matching curve for intermediate region. Ω_B is the value of Ω_e when the target electrons are treated as free, as in eq. (1).

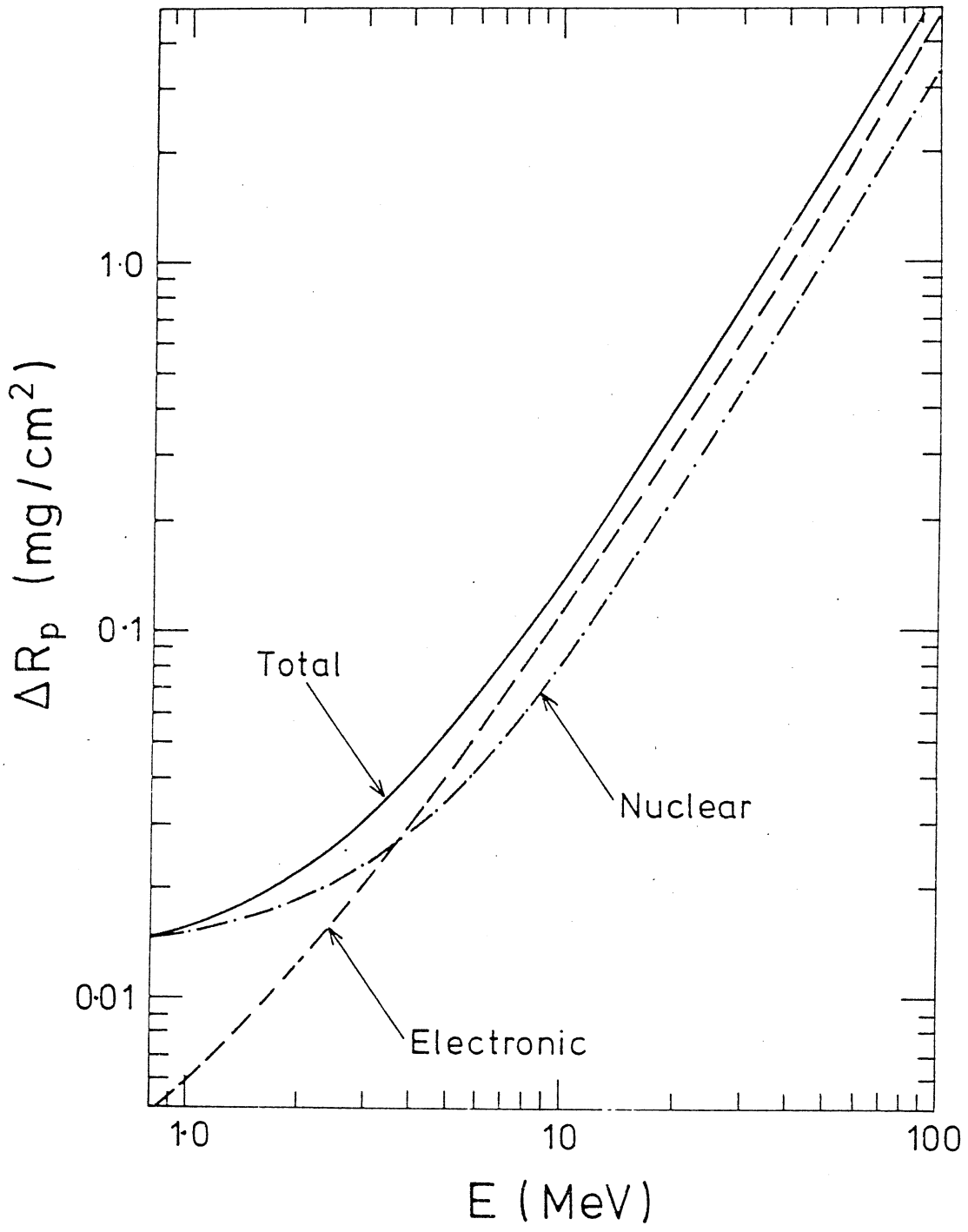

AERE - R 10045 Fig. 3

Projected range straggling of ^{4}He in C as a function of ^{4}He incident energy.